Available online at www.sciencedirect.com
ScienceDirect
Bioorganic & Medicinal Chemistry
Bioorganic & Medicinal Chemistry 15 (2007) 4585–4594

Explaining cyclodextrin–mycotoxin interactions using a 'natural' force field

Alessio Amadasi,[a] Chiara Dall'Asta,[b] Gianluigi Ingletto,[c] Roberto Pela,[b] Rosangela Marchelli[b] and Pietro Cozzini[c,*]

[a]Department of Biochemistry and Molecular Biology, University of Parma, I-43100 Parma, Italy
[b]Department of Organic and Industrial Chemistry, University of Parma, I-43100 Parma, Italy
[c]Molecular Modelling Laboratory, Department of General Chemistry, University of Parma, Viale G.P. Usberti, 17/A, I-43100 Parma, Italy

Received 15 November 2006; revised 3 April 2007; accepted 5 April 2007
Available online 10 April 2007

Abstract—Docking techniques and the HINT (Hydropathic Interaction) program were used to explain interactions of aflatoxin B_1 and ochratoxin A with β- and γ-cyclodextrins. The work was aimed at designing a chemosensor to identify very low concentrations of these mycotoxins by exploiting the affinity of the cyclodextrin cavity for many small organic molecules. Actually, the inclusion of the fluorescent portion of these toxins into the cavity may lower the quenching effect of the solvent, thus enhancing the luminescence. HINT is a 'natural' force field, based on experimentally determined Log $P_{octanol/water}$ values, that is able to consider both enthalpic and entropic contributions to the binding free energy with an unified approach. HINT is normally applied to predict the $\Delta G°$ of binding for protein–ligand, protein–protein, and protein–DNA interactions. The leading forces in biomolecular processes are the same as those involved in organic host–guest inclusion phenomena, therefore we applied this methodology for the first time to cyclodextrin complexes. The results allowed us to explain spectroscopic data in absence of available crystallographic or NMR structural data.

1. Introduction

Aflatoxins B_1 (AFB1) (Fig. 1a), B_2, G_1, G_2 are natural substituted coumarins produced by *Aspergillus flavus*, *Aspergillus nomius*, and *Aspergillus parasiticus*, which can be found on foodstuffs supporting fungal growth, such as cereals, dried fruits, oil seeds, spices, and pulses.[1] These toxins are hepatocarcinogens and mutagen agents and in 1993 they were declared as Group 1 carcinogens by the International Agency for Research on Cancer (IARC).[2]

Ochratoxin A (OTA) (Fig. 1b) is a mycotoxin produced by *Penicillum verrucosum*, *Aspergillus ochraceus,* and other related species, which can be found in cereals, beans, groundnuts, spices, dried fruits, and coffee beans.[3] OTA is nephrotoxic, hepatotoxic, immunosuppressive, teratogenic, and carcinogenic in several animal species and has been classified as a possible carcinogen for humans (Group 2B) by IARC.[4,5]

There has been a recent increase in mycotoxin contamination of foods, causing concern among producers and consumers. Therefore, the availability of reproducible and sensitive methods for screening foodstuffs is essential.

Different analytical methods are currently used for AF screening: immunoassay methods are well suited for a rapid, routine screening, although the detection of concentrations of AFM1 in milk that are very close to the European Union legal limit (50 ng/l) is affected by significant error, due to the low reproducibility and sensitivity of the ELISA technique. Chromatographic methods, in

Abbreviations: AF, aflatoxin; CD, cyclodextrin; CSD, Cambridge Structural Database; ELISA, enzyme-linked immunosorbent assay; HPLC, high performance liquid chromatography; IARC, International Agency for Research on Cancer; LGA, lamarckian genetic algorithm; OTA, ochratoxin A; o.s., operative system; QSAR, quantitative structure–activity relationship; vdW, van der Waals.

Keywords: HINT; Cyclodextrins; Docking; Scoring functions; Mycotoxins.

* Corresponding author. Tel.: +39 0521 905669; fax: +39 0521 905556; e-mail: pietro.cozzini@unipr.it

0968-0896/$ - see front matter © 2007 Elsevier Ltd. All rights reserved.
doi:10.1016/j.bmc.2007.04.006

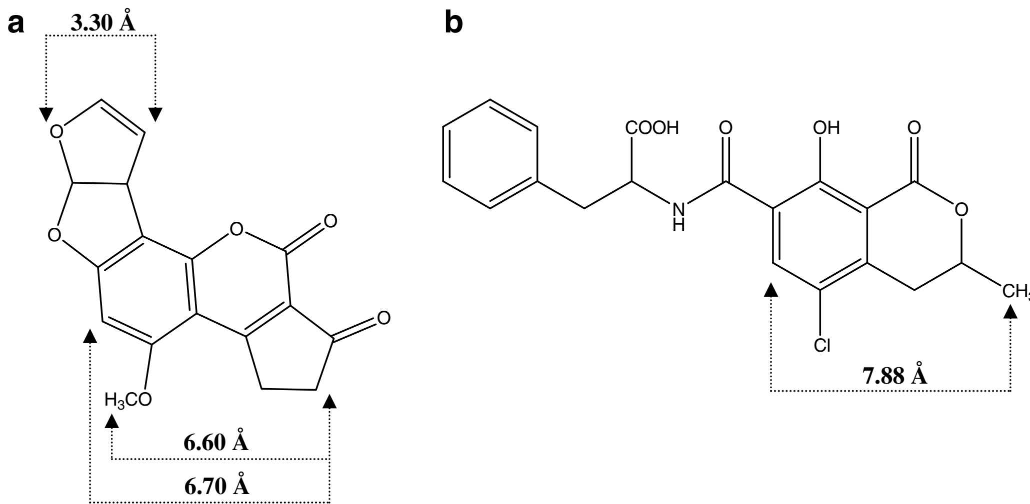

Figure 1. Chemical structures of AFB1 (a) and OTA (b). The distances (atom centre to atom centre) between different extremities of the molecules are highlighted.

particular reversed-phase HPLC with fluorescence detection, are currently the most commonly used and are particularly suited for the analysis of complex matrices. AFs have a rigid, cyclic oxygenated structure with a high degree of conjugation which provides low native fluorescence.[6] While AFB2 and AFG2 are endowed with fairly high fluorescence quantum yield, native fluorescence of AFB1 and AFG1 is low. Native fluorescence may be enhanced by the use of cyclodextrins (CDs), which are cyclic oligosaccharides formed by α-(1,4)-linked glucose units, and which have the form of a hollow truncated cone with a hydrophilic external surface that makes them soluble in water, and a hydrophobic internal cavity, which allows the formation of inclusion complexes.[7] The inclusion of a fluorophore into the cavity generally increases fluorescence emission by protection from the quenching effect exerted by water.[8] β-CD, in particular, has been used either as a post-column additive[9–11] or directly dissolved in the chromatographic mobile phase.[12] Substantial enhancement of fluorescence emission has been reported for AFs with an unsaturated furan ring (AFB1 and AFG1), while the emission properties of AFs with a saturated furan ring (AFB2 and AFG2) have been shown to remain practically unchanged.[11,12]

The development of efficient analytical tools for the detection of OTA is more difficult. OTA is a derivative of isocoumarinic acid linked to L-phenylalanine through an amidic bond, with optical activity and natural fluorescence. The natural fluorescence of OTA is due to the presence of the isocoumarinic moiety, and is enhanced by the presence of a rigid system due to formation of an intramolecular hydrogen bond between the phenolic moiety and the amidic carbonyl (α-form) or the esteric carbonyl group (β-form). Based on previous studies with AFs,[11,12] we attempted to enhance the fluorescence of OTA using CDs, but the results were not significant.

In the present work, we investigated the mechanism of OTA inclusion into CDs by molecular modelling techniques, and tried to better understand the nature of the interactions between AFB1 and CDs, previously studied by Dall'Asta et al. using spectroscopic techniques.[13] The exhaustive comprehension of the AFB1–CD inclusion mechanism, as well as the study of OTA–CD interaction, may lead to the design of chemosensor devices based on fluorescence. The well-known specificity of fluorescent probes would allow for more sensitive and accurate detection of mycotoxins, even at very low concentrations, minimizing the risk of false negative/positive results usually associated with ELISA tests. Moreover, chemosensors based on a luminescence response may be integrated into microarray systems, which could be applied for early detection of post-harvest contamination, providing for an easy-to-use control tool for mycotoxin analysis.

2. Results and discussion

2.1. Preliminary fluorescence experiments

As previously reported by Dall'Asta et al.,[12,13] β-CD and its charged derivative polysuccnyil–β-CD act as fluorescence enhancers for AFs. However, the host–guest complexation cannot be determined by NMR experiments, given the strong toxic, mutagenic, and carcinogenic effects of AFs even at low concentrations. Indeed, the switch-on phenomenon was investigated using spectroscopic techniques (UV and fluorescence) and a probable inclusion model was reported, based on competition experiments. Fluorescence enhancement due to AF–CD complexation was then used for chromatographic determination of AFs, resulting in very good sensitivity.[12]

A preliminary study was conducted to enhance fluorescence of OTA using CDs. Structurally, OTA is formed by an isocoumarinic moiety (Fig. 1b), which is responsible for its low native fluorescence, linked through an amidic bond to a phenylalanine residue. Thus, interaction between OTA and CDs may involve the isocou-

Table 1. Fluorescence enhancement recorded for AFB1 and OTA with α-, β-, and γ-CD

Complex	F/F_0
AFB1–α-CD	5.7 ± 0.1
AFB1–β-CD	11.6 ± 0.2
AFB1–γ-CD	2.5 ± 0.3
OTA–α-CD	1.0 ± 0.1
OTA–β-CD	1.2 ± 0.2
OTA–γ-CD	0.99 ± 0.1

The data are reported as F/F_0, where F_0 is the native fluorescence of the mycotoxin and F is the fluorescence obtained using cyclodextrin (molar ratio: mycotoxin/CD, 1:10^5).

marinic portion as well as the phenylic moiety, but fluorescence enhancement should be observed only in the former case.

α-, β-, and γ-CDs were tested for both AFB1 and OTA, according to their cavity dimensions, in order to establish which CD gave the best enhancement for each mycotoxin. As reported in Table 1, emission of AFB1 was switched on using α-, β-, and γ-CD, whereas no significant enhancement was observed for OTA.

Fluorescence enhancement usually occurs when complexation into the CD protects the fluorophore from solvent quenching. On the contrary, emission cannot be switched on if the fluorescent system remains outside of the cavity. The inclusion of the isocoumarinic portion, which is responsible for OTA fluorescence, seems to be unlikely, based on spectroscopic data.

Starting from these observations, the interaction between CDs, AFB1, and OTA was studied using molecular modelling, in order to further investigate AF–CD and OTA–CD complexation.

2.2. The 'natural' HINT force field

Many computational studies of guest inclusion in CDs have been reported over the past several decades and they are well reviewed by Lipkowitz.[14] The vast majority of these studies, with the exception of QSAR models,[15,16] have reported molecular dynamics simulations or molecular mechanical calculations, based on widely used Newtonian force fields.[17,18] Very recently, quantum chemistry calculations on AFB1–β-CD inclusion complexes have also been reported.[19] In the present work, we propose a different approach to investigate the mechanism of OTA and AFB1 inclusion into CDs. Our analysis was carried out using two docking packages, GOLD[20] and AutoDock,[21] and the HINT program as a post-process scoring function (see Section 4). HINT is a 'natural' force field, based on experimentally determined Log $P_{\text{octanol/water}}$ values.[22,23] High HINT scores are indicative of a good interaction (negative $\Delta G°$), while low scores are indicative of a weak interaction between the examined molecules. HINT is normally applied to predict the $\Delta G°$ of binding for biological interactions such as protein–ligand, protein–protein, protein–DNA, and protein–water.[22,24–29] Non-covalent interactions involved in inclusion phenomena are the same as those involved in biomolecular recognitions. Therefore, we believe that HINT could be extremely useful in computational studies of host–guest complexation. Indeed, because Log $P_{o/w}$ is derived from a solvation–desolvation experiment, HINT implicitly includes entropic contributions arising from water molecule displacement during complex formation, whereas the classical molecular mechanics approach usually omits, or only partially evaluates, solvation/desolvation events.[23] It follows that HINT may be particularly suitable for the evaluation of entropically driven hydrophobic effects, which are among the main driving forces of CD inclusion phenomena.[7,14,16]

2.3. Docking studies

β-CD, γ-CD, AFB1, and OTA structures were taken from the Cambridge Structural Database (CSD) and prepared for docking as described in Section 4. Docking was performed using GOLD and AutoDock. Both these programs allow full ligand flexibility but consider the host as rigid, therefore the CD molecule geometry was kept fixed in the crystal conformation reported in CSD. All the 50 docking poses generated by GOLD and the 100 generated by AutoDock for each ligand were re-scored with HINT. Among the 50 solutions generated by GOLD for each mycotoxin–CD complex, two were carefully analyzed. The solution with the best energy assigned by the ChemScore scoring function[30] included within the GOLD package (for convenience we will refer to it as best ChemScore), and the one with the highest HINT score (best HINT/GOLD). Similarly, of the 100 solutions proposed by AutoDock, the one with the AutoDock best energy and the one with the highest HINT score were selected (we will refer to them as best AutoDock and best HINT/AutoDock, respectively).

A consensus approach, combining different docking tools and scoring functions based on different concepts, should allow a more reliable analysis of the inclusion mechanism, overcoming errors and approximations of each single molecular modelling tool.

2.4. Predicted binding modes

2.4.1. AFB1 in β-CD. The four best solutions selected by the scoring functions described above exhibit the furan moiety of AFB1 inserted into the CD cavity, with the coumarinic ring protruding into the solvent through the wider edge of the truncated cone (Fig. 2a). However, the coumarinic ring is bent towards the border of the cavity, allowing hydrogen bond formation between AFB1 carbonyl groups and CD secondary hydroxyl groups. Best AutoDock, best HINT/AutoDock, and best HINT/GOLD solutions do not display significant differences (the rmsd between the three proposed ligand conformations are below 0.75 Å). On the other hand, the best ChemScore solution, coloured in magenta in Figure 2a, is rotated in comparison with the others. This difference is due to the formation of hydrogen bonds with different secondary hydroxyl groups, located on the CD's wider edge, but the predicted inclusion

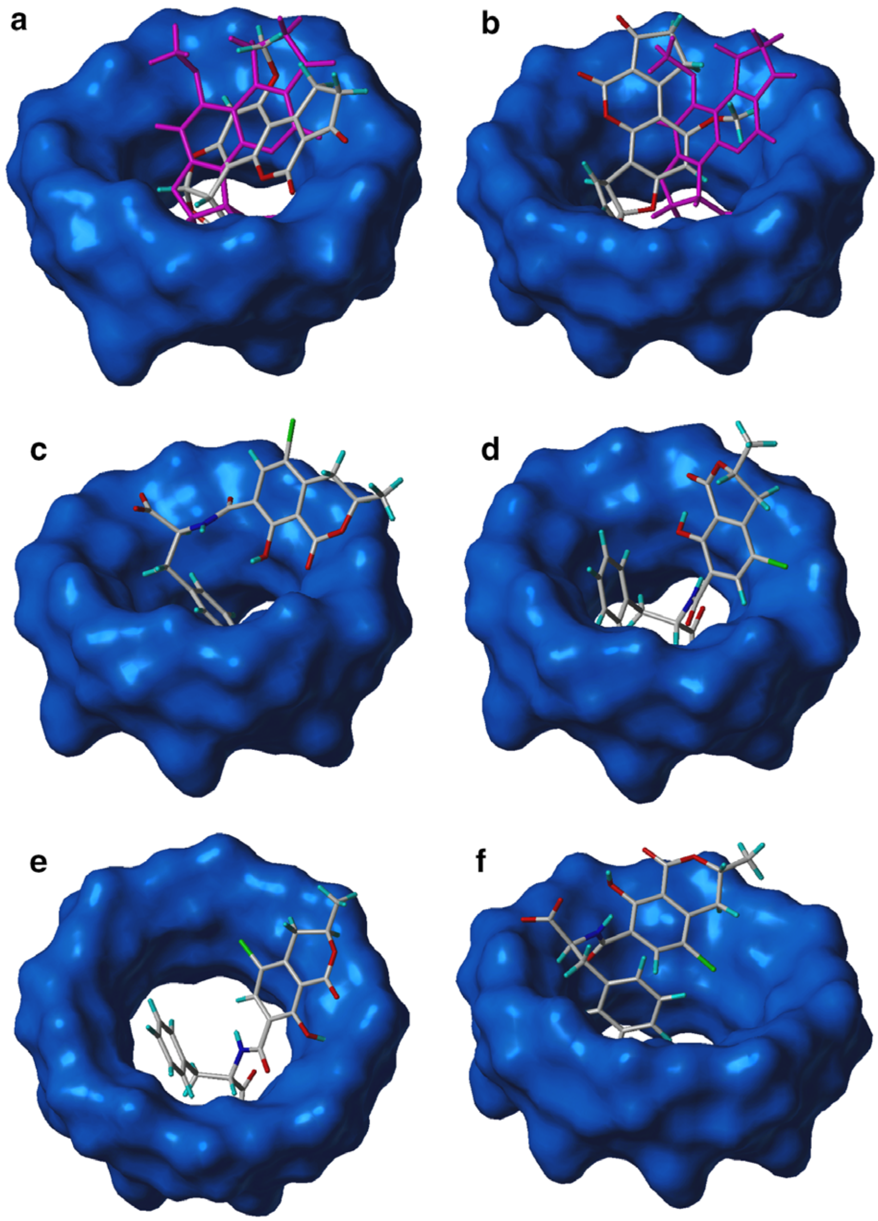

Figure 2. Illustrations showing the predicted inclusion mechanisms of AFB1 and OTA into β- and γ-CDs. The Connolly surface of the host (CD), built using Sybyl MOLCAD tools, is coloured blue, while guest molecules (mycotoxins) are rendered in capped sticks. (a) Best HINT/GOLD and best ChemScore (magenta) for AFB1 in β-CD. (b) Best HINT/AutoDock and best HINT/GOLD (magenta) for AFB1 in γ-CD. (c) Best HINT/GOLD for OTA in β-CD. (d) Best HINT/AutoDock for OTA in β-CD. (e) Best HINT/GOLD for OTA in γ-CD. (f) Best HINT/AutoDock for OTA in γ-CD.

mechanism is the same, with the furan moiety of AFB1 inserted into the CD cavity.

2.4.2. AFB1 in γ-CD. Best ChemScore and best HINT/GOLD solutions predicted an inclusion mechanism of AFB1 into γ-CD that is analogous to the one proposed for the inclusion in β-CD. The furan moiety is inserted into the CD cavity, while the coumarinic ring and the cyclopentanone ring are more exposed to the solvent, allowing hydrogen bond formation between their carbonyl groups and secondary hydroxyl groups located around the CD's wider opening (Fig. 2b, magenta). Best AutoDock and best HINT/AutoDock solutions are very similar to each other (the rmsd between the two solutions is below 0.75 Å), but show differences with the best ChemScore and the best HINT/GOLD. Their predicted binding mode also exhibits, in addition to the furan moiety, the coumarinic phenyl ring and its methoxy group partially inserted into the cavity (Fig. 2b).

2.4.3. OTA in β-CD. The docking of OTA was carried out with the phenolic group in both the protonated and deprotonated forms, in agreement with its experimental pK_a of 7.1. The two forms did not display differences regarding the inclusion mechanism, while different binding free energies were predicted (Table 2 reports a mean $\Delta G°$ value).

Table 2. HINT scores and predicted binding free energies (kcal mol^{-1}) calculated by ChemScore and AutoDock, relative to the best docking solutions selected for different mycotoxin–CD complexes

	Best HINT/GOLD	Best HINT/AutoDock	Best ChemScore	Best AutoDock
AFB1–β-CD	1496	979	−7.22	−6.98
AFB1–γ-CD	1363	862	−6.21	−6.23
OTA–β-CD	3881	2553	−9.05	−5.77
OTA–γ-CD	1403	2292	−6.77	−5.50

When used to dock OTA into β-CD, different docking-scoring combinations produced different predictions. The two suggested alternative mechanisms of OTA inclusion into β-CD are shown in Figure 2c and d, respectively. Best ChemScore and best HINT/GOLD solutions (Fig. 2c) show the phenyl ring of L-phenylalanine inserted into the CD cavity, while the carboxylic function and the isocoumarinic ring protrude into the solvent towards the wider opening. In this way the carboxylate on the phenylalaninic residue and the phenolic and ester carbonyl groups on the isocoumarinic ring can form hydrogen bonds with secondary hydroxyl groups placed on the CD's hydrophilic edge. Best AutoDock and best HINT/AutoDock solutions (Fig. 2d), on the contrary, show the whole phenylalaninic portion inserted into CD cavity, with the carboxylate group exposed to the solvent through the narrower edge of the hollow truncated cone. However, once again the isocoumarinic ring is not placed within the CD cavity, but is more exposed, allowing hydrogen bond formation between its carbonyl group and CD's secondary hydroxyl groups.

2.4.4. OTA in γ-CD. Best ChemScore, best HINT/GOLD and best HINT/AutoDock solutions are in agreement regarding the inclusion of OTA into γ-CD. The predicted binding mode matches the one selected by AutoDock and HINT/AutoDock as best docking result for OTA inclusion in β-CD. The phenylalaninic portion is inserted into the CD cavity, with the exception of the carboxylate group, which is exposed to the solvent through the narrower opening of γ-CD. The isocoumarinic ring is exposed to the solvent, allowing hydrogen bond formation between its carbonyl group and secondary hydroxyl groups around the wider CD opening (Fig. 2e). The best HINT/AutoDock solution shows, however, a very different behaviour (Fig. 2f). Only the phenylalanine phenyl group and, partially, the chlorine on the isocoumarinic ring are included into the CD hole, while the entire molecule lies on the boundary of the CD's wider edge, allowing hydrogen bond formation between OTA hydrophilic groups (carboxylate, carbonyl, and phenolic-OH) and CD hydroxyl groups.

2.5. Predicted binding free energies

The AutoDock and ChemScore predicted free energy of binding (kcal mol^{-1}) and the HINT scores (the higher the HINT score the lower the predicted $\Delta G°$) for the best solutions selected by each program for different CD–mycotoxin complexes are reported in Table 2. The calculation of absolute binding free energies is very challenging, while the predicted free energy can be more properly used in relative comparison between different guest molecules or different binding poses of the same molecule ($\Delta\Delta G°$). Furthermore, the HINT program is particularly suitable for the evaluation of solvation/desolvation events, critical in inclusion phenomena. Therefore, our discussion will focus mainly on HINT calculated free energies with particular attention to predicted $\Delta\Delta G°$. Previous studies[22] have reported that about 500 HINT score units correspond to a $\Delta\Delta G°$ of -1 kcal mol^{-1} and this value has been shown to have general validity, being consistent with experimental findings in different heterogeneous systems.[22,24–29]

2.6. Post-docking analysis

2.6.1. AFB1. As water molecule displacement and hydrophobic interactions are probably the main driving forces of CD inclusion phenomena,[7,14,16] we performed a careful mapping of the hydrophobic–hydrophilic properties of examined guest molecules using HINT. Figure 3 shows HINT hydrophobic-polar contour maps of AFB1 and OTA. The region of AFB1 exhibiting the most hydrophobic character is constituted by the methoxy group and by the portion of the coumarinic and cyclopentanone ring opposite to the carbonyl groups. However, the methoxy group alone is probably too small to produce a good fitting, displacing all water molecules placed within the β-CD cavity. The hydrophobic portion of coumarinic and cyclopentanone rings cannot be included into β-CD for steric reasons. As shown in Figure 1a, the measured distances (centre atom to centre atom) between the extremities are beyond 6.40 Å. The additional increase in size given by vdW radius makes the inclusion of this part of AFB1 into β-CD impossible due to a cavity diameter of between 6.0 and 6.5 Å.[7] On the contrary, the furan moiety has a size that allows a good fitting into the cavity (the measured distance between the extremities is 3.30 Å) and it is also hydrophobic in the portion opposite to the oxygen atoms (see Fig. 3a). These considerations support the inclusion mechanism proposed by all the employed molecular modelling tools for AFB1 into β-CD. Furthermore, the mechanism agrees with previous experimental results obtained by Dall'Asta et al. using spectroscopic techniques[13] and is consistent with the observed enhancement of AFB1 fluorescence emission in presence of β-CDs.[8,10–12]

γ-CD exhibits a cavity diameter between 7.5 and 8.3 Å[7] which allows for a different way of binding for AFB1, such as the one shown by the best AutoDock and the

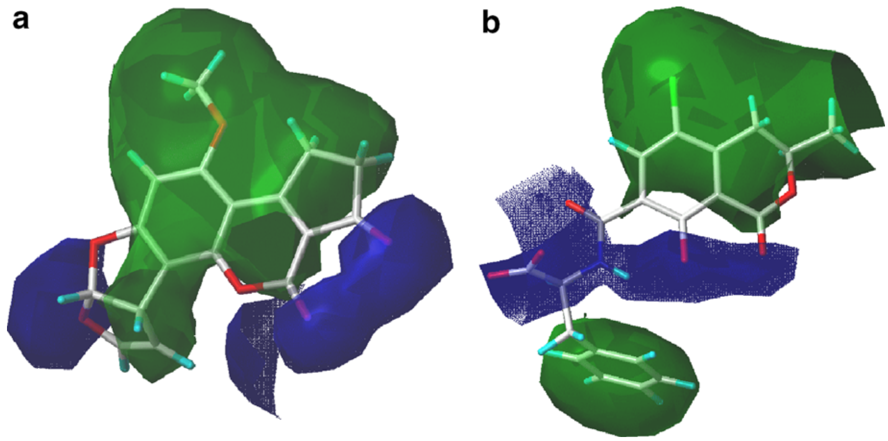

Figure 3. HINT hydrophobic-polar contour maps of AFB1 (a) and OTA (b). Hydrophobic regions are coloured green, while hydrophilic regions are coloured blue. The two molecules are rendered in capped sticks.

best HINT/AutoDock solutions. However, the assigned HINT score favours the HINT/GOLD best solution (1363 for best HINT/GOLD vs 862 for best HINT/AutoDock). This difference of about 500 HINT score units corresponds to about $-1\ \text{kcal mol}^{-1}$. Thus, among all the docking modes generated by GOLD and AutoDock, HINT considers the one with the furan moiety inserted into the γ-CD cavity as the most energetically favourable, similar to that shown for β-CD. The difference between the highest HINT score associated to AFB1 inclusion into β-CD (best HINT/GOLD) and γ-CD (best HINT/GOLD) is only 133 score units ($\sim -0.25\ \text{kcal mol}^{-1}$). AFB1 inclusion into β-CD is predicted to be slightly more favourable than its inclusion in γ-CD. This finding is in agreement with the free energy calculations made by AutoDock and ChemScore scoring functions, which did not predict $\Delta\Delta G°$ beyond $-1\ \text{kcal mol}^{-1}$ (see Table 2), but it seems to be in contrast with experimental evidence that shows no significant enhancement of AFB1 fluorescence emission in the presence of γ-CD (see Table 1). It should be pointed out that calculated thermodynamic values may contain wide margins of error and this could explain disagreement between calculations and experimental data.[31]

In order to localize potential water sites within complexes generated by docking, we performed an analysis using the software GRID.[32] The GRID water probe did not identify energetically favourable water sites within the CD cavity of the AFB1–β-CD complex, indicating that all the water molecules are displaced and the inclusion mechanism produces a perfect fit. On the contrary, GRID analysis located water molecules in the CD cavity of AFB1–γ-CD complex. This finding suggests that AFB1 inclusion into γ-CD should be less energetically favourable than the inclusion in β-CD, due to the fact that some water molecules are not displaced during ligand binding, because of the cavity's larger size. Furthermore, we can speculate that γ-CD's cavity may not be able to completely protect included AFB1 from the quenching effect exerted by water.

2.6.2. OTA. Both of the two predicted mechanisms of inclusion into β-CD (Fig. 2c and d) can be explained in light of the size and the hydrophobic-polar balance of the OTA molecule. Figure 3b shows the OTA regions that display a more hydrophobic character, while in Figure 1b several distances between different extremities of the OTA molecule are highlighted. The entire hydrophobic portion of the isocoumarinic ring cannot be included into β-CD for steric reasons (the measured distance, centre atom to centre atom, between the aromatic hydrogen atom and a hydrogen belonging to the methyl group is of 7.88 Å), while the highly hydrophobic chlorine atom alone is probably too small to allow a good fitting into the cavity. Therefore, the inclusion of the hydrophobic L-phenylalanine phenyl ring, which allows hydrogen bond formation between OTA hydrophilic groups and CD secondary hydroxyl groups, seems to be realistic. Indeed, this predicted inclusion mechanism exhibits a HINT score of 3881, against a score of 2553 assigned to the OTA conformation displaying the whole phenylalaninic portion inserted into the CD cavity (corresponding to a $\Delta\Delta G°$ of more than $-2\ \text{kcal mol}^{-1}$). The lower predicted affinity for the latter solution may be due to the inclusion of the hydrophilic amidic portion of L-phenylalanine into the hydrophobic CD cavity, but also to a more difficult hydrogen bond formation between the OTA carboxylate group and the primary hydroxyl groups located around the narrower opening of the β-CD cavity. These hydroxyl groups are not orientated towards the interior of the hole. The predicted $\Delta\Delta G°$ between HINT best solutions for the OTA–β-CD complex (best HINT/GOLD) and the AFB1–β-CD complex (best HINT/GOLD) is about $-4.5\ \text{kcal mol}^{-1}$. This is consistent with a stronger binding of OTA than AFB1 to β-CD, that can be justified by the higher number of hydrogen bonds formed by OTA and particularly by its negatively charged carboxylate group (which should contribute to stronger interactions with CD hydroxyl groups, due to the Coulombic reinforcement). This finding suggests that the experimentally observed lack of fluorescence emission enhancement for OTA in presence of β-CD is probably due to the nature of the inclusion mechanism and not to weak binding. Indeed, the isocoumarinic ring responsible for OTA fluorescence is probably not included in the hydrophobic cavity and, thus, not protected by the quenching effect exerted by water.

The predicted inclusion mechanism of OTA into γ-CD is also not supportive for a possible fluorescence enhancement using this host. Neither of the two alternative predicted modes of binding (best ChemScore, best AutoDock and best HINT/GOLD, shown in Fig. 3e, and best HINT/AutoDock, shown in Fig. 3f) displays the isocoumarinic ring inserted within the CD cavity. Furthermore, it should be noticed that the calculated HINT scores are lower than those for OTA inclusion into β-CD (see Table 2). The proposed model seems justified by the size of γ-CD (diameter of 7.5–8.3 Å), which, although greater than β-CD, is not wide enough to accommodate the isocoumarinic ring.

The GRID water probe did not identify energetically favourable water sites within the CD cavity of the OTA–β-CD complex, while it was able to detect different potential water sites within the CD cavity of the OTA–γ-CD complex. In a practical sense, γ-CD seems too small to include the isocoumarinic ring, but too large to produce a good fitting with the phenylalanine phenyl ring by displacement of all the water molecules.

2.7. Circular dichroism experiments

As discussed above, molecular modelling simulations show that complexation of OTA with β-CD likely occurs through the inclusion of the phenylalanine residue. This model is in agreement with experimental fluorescence results: in the complex, the isocoumarinic nucleus is still exposed to solvent quenching and, thus, emission remains unchanged. Nonetheless, the inclusion of the phenyl ring should cause changes in the circular dichroism spectrum at 230–280 nm, which is the typical range of phenylalanine UV absorption.

The inclusion of the bifuranic system of AFB1 into the β-CD cavity allows for fluorescence enhancement due to the protection of the fluorophore from the quenching and also in this case a variation in the circular dichroism spectrum would be expected.

In order to prove the proposed inclusion model for both AFB1–β-CD and OTA–β-CD complexes, circular dichroism experiments were performed. The spectra were acquired for aqueous solutions of OTA, AFB1, and β-CD, and the same experiments were repeated for aqueous solutions of AFB1 + β-CD and OTA + β-CD (molar ratio: toxin/β-CD, 1:10^5). The results are reported in Figure 4a and b.

The circular dichroism signal of β-CD was not significantly different from the baseline. We, therefore, decided to compare the spectra obtained for the complexes with those registered for AFB1 or OTA in aqueous solution. As reported in Figure 4a, both the bands in the circular dichroism spectrum obtained for the AFB1–β-CD complex are stronger than those observed for AFB1. These data suggest that the inclusion of AFB1 in the βCD cavity involves the bifuranic system, which is responsible for absorption at 350–380 nm. The slight changes in the circular dichroism signals may be explained by several considerations. First, since the AFB1–β-CD binding constant is low, a strong interaction signal cannot be expected. Second, we could not use the same molar ratio between toxin and CD that was used in the fluorescence measurements. Given the low solubility of β-CD in water, only the toxin concentration was increased in order to obtain good UV absorption, as required for the experiment.

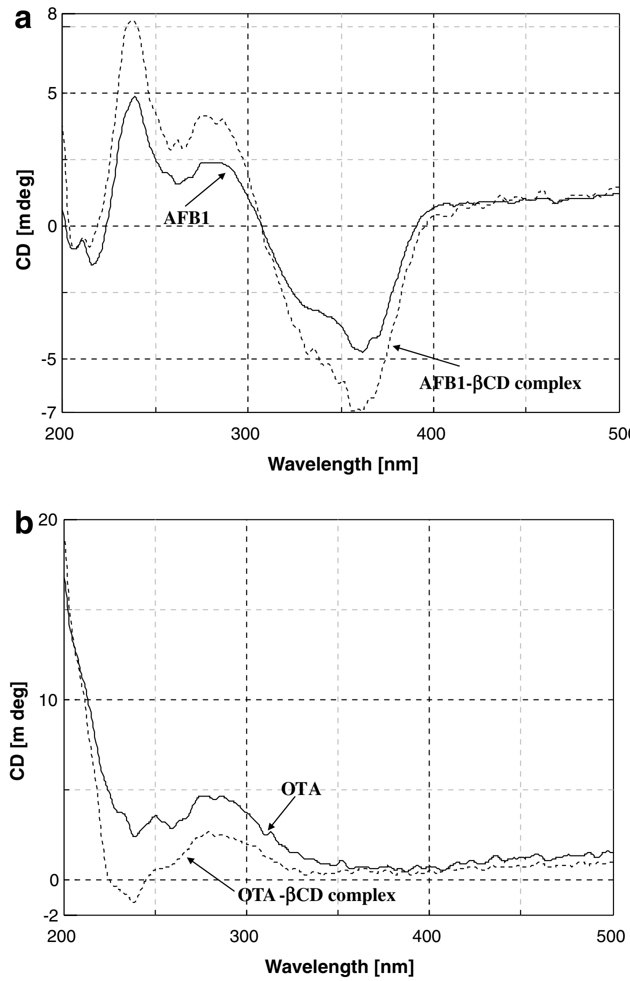

Figure 4. Comparison between the circular dichroism spectra recorded for AFB1 and the inclusion complex AFB1–β-CD (a) and for OTA and the inclusion complex OTA–β-CD (b).

The circular dichroism signal of the OTA–β-CD complex, reported in Figure 4b, did not differ significantly from the OTA signal in the typical absorption range of the isocoumarinic moiety (330–380 nm), while small variation was observed at 250–280 nm, where phenyl ring absorption occurs. Although the change in the band is not strong, according to the low stability constant expected for this complex, these data support the inclusion of the phenylalanine residue of OTA suggested by molecular modelling. The suggested binding between the phenylalanine residue of OTA and the CD cavity is promising for the design of a chemosensor for OTA detection. Unfortunately, the interaction between OTA and β-CD is probably too low to allow a specific recognition. The synthesis of new positively charged CDs may lead to a more specific inclusion of OTA into the cavity.

Moreover, functionalization of the CD with a suitable fluorophore, able to furnish energy transfer to OTA, could be considered. The increased binding between modified β-CD and the phenyl ring of OTA, as well as the interaction between the positive charges on the CD ring and the carboxylated group of the mycotoxin, could be used to drive the guest into the right position, allowing for energy transfer phenomena.

3. Conclusions

In conclusion, we tried to explain the inclusion mechanism of AFB1 and OTA into β- and γ-CDs in the absence of available crystallographic or NMR structural data, using molecular modelling approaches imported from the field of protein–ligand docking. The proposed mechanism of inclusion allows to explain data previously reported on fluorescence emission enhancement for AFB1 in presence of β-CDs[8,10–12] and supports the conclusions achieved by Dall'Asta et al. using spectroscopic techniques.[13] Furthermore, in this study we suggest for the first time a binding between the phenylalanine portion of OTA and the CD cavity. Experimental data showed that the affinity of AFs to β-CD is rather low, being the calculated binding constants for the AF:CD complexes around 10^{-3} M.[13] Although the enhancement of AFs native fluorescence, due to inclusion into CDs, has already been successfully employed in HPLC analysis for increasing the sensitivity,[12] the low affinity of the formed complex cannot lead to a specific chemosensor for mycotoxin detection in a complex matrix such as food. However, the understanding of the inclusion mechanism may allow to design more specific CDs, which will be functionalized in order to increase the affinity to the guests (AFs, OTA, or other mycotoxins), allowing their possible use as chemosensors.

4. Experimental

The program Sybyl version 7.0 (Tripos, Inc., St. Louis, MO, USA; www.tripos.com), used in the study, was installed on a FUEL Silicon Graphics workstation running o.s. IRIX 6.5. The program HINT 3.09 β test version was used as an add-on module within Sybyl. This version of HINT was developed by Prof. G.E. Kellogg and can be obtained from eduSoft (eduSoft, LC, Ashland, VA, USA; www.edusoft-lc.com). The GOLD version 2.2 (CCDC, Cambridge, UK; www.ccdc.cam.ac.uk) and the AutoDock version 3.0 (SCRIPPS, La Jolla, CA, USA; www.scripps.edu) programs were installed on a dual pentium processor, running o.s. Linux Red Hat Enterprise 3.0.

4.1. Reagents

AF and OTA standards were from SIGMA (St. Louis, MO, USA). Bidistilled water was produced using an Alpha-Q System Millipore (Marlborough, MA, USA). α-, β-, and γ-CD were purchased from ACROS (Carlo Erba, Italy). Working solutions of mycotoxins (10^{-7} M) and of mycotoxins with CDs (10^{-2} M) were prepared by dissolving the proper amount of powder standard and CD in water and were stocked at −4 °C for a month. Decontamination of waste solutions and glassware was performed with sodium hypochlorite (10% aqueous solution) for 12 h.

4.2. Spectroscopic experiments

Fluorescence spectra were recorded on a Perkin-Elmer LS55 instrument in a 0.2 × 1.0-cm quartz cell. The excitation wavelengths were 365 and 380 nm for AFB1 and OTA, respectively. The emission scan was performed in the range 400–600 nm. Both emission and excitation slits were set at 15 nm. Each spectrum was recorded in triplicate. Circular dichroism spectra were recorded on a JASCO J-715 spectropolarimeter equipped with a Peltier thermostat (measurements done at 25 °C): acquisition range 200–500 nm, accumulations 3, band width 1.0 nm, response 1 s, scan speed 100 nm/min. Quartz cells (0.1 × 1 cm) were used. All spectra were treated with the noise reduction software included in the program J-700 for Windows Standard Analysis, version 1.33.00.

4.3. Host and guest preparation for docking

The three-dimensional coordinates of β-CD, γ-CD, AFB1, and OTA were taken from CSD (www.ccdc.cam.ac.uk) (Ref. code: BCDEXD03, NUNRIX, AFLATC, and JAZDUJ, respectively) and imported into the molecular modelling program Sybyl.

All structures were checked for chemically consistent atom and bond type assignment. Hydrogen atoms were added using Sybyl Build/Edit menu tools. To avoid steric clashes, added hydrogen atoms were energy-minimized using the Powell algorithm, with a convergence gradient of 0.5 kcal mol^{-1} for 1500 cycles. This procedure affected only non-experimentally detected hydrogen atoms.

4.4. Gold

The CDs and the ligands were prepared for docking using Sybyl (see above). All hydrogen atoms were added to the CDs and to the ligands and all water molecules were removed from the target structure. The input files for docking were generated in .mol2 format. We used a radius of 15.0 Å from the centre of the CD cavity to direct site location. For each of the genetic algorithm runs, a maximum number of 100,000 operations were performed on a population of 100 individuals with a selection pressure of 1.1. Operator weights for crossover, mutation and migration were set at 95, 95, and 10, respectively, as recommended by the software authors. The number of islands was set to 5 and the niche size was set to 2. 50 GA runs were performed in each docking experiment. The ChemScore fitness function, implemented in GOLD, was used to identify the better binding mode. ChemScore is an empirical scoring function.[30] The overall binding free energy is composed of several free energy terms (hydrogen bonding, hydrophobic interactions, entropic changes, etc.) and the coefficients of each term in the sum are derived from fitting to known experimental binding energies.

4.5. AutoDock

The CDs were treated using the united atom approximation. Only polar hydrogens were added to the structure and atomic charges were then calculated using the Gasteiger method.[33] All water molecules were removed from the target structure. $60 \times 60 \times 60$ Å affinity grids, centred on the CD cavity with 0.375 Å spacing, were calculated by use of Autogrid 3.0,[21] for each of the following atom types: C, A (aromatic C), N, O, S, H, and Cl.

Only polar hydrogens were added to the ligands (AFB1 and OTA) and Gasteiger charges were assigned. The rotatable bonds were selected via AutoTors.[21]

We selected the Lamarckian genetic algorithm (LGA) for ligand conformational searching. LGA adds local minimization to the genetic algorithm, enabling modification of the gene population.[21] The following docking parameters were used: trials of 100 dockings, population size of 100, random starting position and conformation, translation step ranges of 1.0 Å, rotation step ranges of 1.0 Å, elitism of 1, mutation rate of 0.02, crossover rate of 0.8, local search rate of 0.06 and 250,000 energy evaluations.

4.6. Hydropathic analysis

We used the HINT (Hydropathic Interactions) software[23,34] as a post-process scoring function. All the 50 docking poses generated by GOLD and the 100 generated by AutoDock for each ligand were re-scored with HINT and the solution exhibiting the highest HINT score (the higher the HINT score, the lower the negative binding free energy variation), was selected as the best docking model for HINT. HINT first calculates Log $P_{o/w}$ (partition constant for 1-octanol/water) for each component of the complexes. The Log $P_{o/w}$ of a molecule is the sum of all hydrophobic atomic constants, **a**, for that molecule. HINT assigns to each interacting atom a partial Log $P_{o/w}$ value $\mathbf{a_i}$ and a Solvent Accessible Surface $\mathbf{S_i}$. For both CDs and ligands the partitions were performed using the calculate method, an adaptation of the CLOG-P method of Leo.[35] The 'essential' option was chosen to perform molecule partition. With this approach only polar hydrogens are treated explicitly.

Genetic algorithms fulfil the role of global search particularly well, but are not always suited for local optimisation.[21] To allow a more accurate evaluation of the binding free energy, a local optimisation of the ligand and CD rotatable bonds, based on the HINT score, was performed after docking. This optimisation generally affected hydroxyl groups on the CDs.

4.7. Grid

The GRID program (www.moldiscovery.com)[32] was used to propose water molecule sites within host–guest complexes generated by docking. The standard water probe was applied over the region of interest, that is, a box measuring $15 \times 15 \times 15$ Å centred on the ligand within the CD cavity. The grid spacing was set to 0.33 Å.

Acknowledgments

We gratefully acknowledge Prof. D.J. Abraham and Prof. G.E. Kellogg (Virginia Commonwealth University) for the HINT software.

References and notes

1. Leitao, J.; De Saint Blanquat, G.; Bailly, J. R.; Paillas, C. H. *J. Chromatogr.* **1988**, *435*, 229.
2. In *IARC Monographs on the Evaluation of Carcinogenic Risks to Humans.* International Agency for Research on Cancer: Lion, France, 1993; Vol. 56, p 489.
3. The Third FAO/WHO/UNEP International Conference on Mycotoxins; MYC-CONF/99/5c, 1999.
4. Shier, W. T.; Shier, A. C.; Xie, W.; Mirocha, C. J. *Toxicon* **2001**, *39*, 1435.
5. Hussein, H. S.; Brasel, J. M. *Toxicol* **2001**, *167*, 101.
6. Holcomb, M.; Wilson, D. M.; Trucksess, M. W.; Thompson, H. C. *J. Chromatogr.* **1992**, *624*, 341.
7. Loftsson, T.; Brewster, M. E. *J. Pharm. Sci.* **1996**, *85*, 1017.
8. Vazquez, M. L.; Cepeda, A.; Prognon, P.; Mahuzier, G.; Blais, J. *Anal. Chim. Acta* **1991**, *255*, 343.
9. Franco, C. M.; Fente, C. A.; Vazquez, B. I.; Cepeda, A.; Mahuzier, G.; Prognon, P. *J. Chromatogr. A* **1998**, *815*, 21.
10. Francis, O. J.; Kirschenheuter, G. P.; Ware, G. M.; Carman, A. S.; Kuan, S. S. *J. Assoc. Off. Anal. Chem.* **1988**, *7*, 725.
11. Cepeda, A.; Franco, C. M.; Fente, C. A.; Vazquez, B. I.; Rodriguez, J. L.; Prognon, P.; Mahuzier, G. *J. Chromatogr. A* **1996**, *721*, 69.
12. Chiavaro, E.; Dall'Asta, C.; Galaverna, G.; Biancardi, A.; Gambarelli, E.; Dossena, A.; Marchelli, R. *J. Chromatogr. A* **2001**, *937*, 31.
13. Dall'Asta, C.; Corradini, R.; Ingletto, G.; Galaverna, G.; Marchelli, R. *J. Incl. Phenom. Macr. Chem.* **2003**, *45*, 257.
14. Lipkowitz, K. B. *Chem. Rev.* **1998**, *98*, 1829.
15. Suzuki, T. *J. Chem. Inf. Comput. Sci.* **2001**, *41*, 1266.
16. Katritzky, A. R.; Fara, D. C.; Yang, H.; Karelson, M.; Suzuki, T.; Solov'ev, V. P.; Varnek, A. *J. Chem. Inf. Comput. Sci.* **2004**, *44*, 529.
17. Yap, K. L.; Liu, X.; Thenmozhiyal, J. C.; Ho, P. C. *Eur. J. Pharm. Sci.* **2005**, *25*, 49.
18. Zheng, Y.; Haworth, I. S.; Zuo, Z.; Chow, M. S.; Chow, A. H. *J. Pharm. Sci.* **2005**, *94*, 1079.
19. Ramirez-Galicia, G.; Garduno-Juarez, R.; Vargas, M. G. *Photochem. Photobiol. Sci.* **2006**, *6*, 110.
20. Jones, G.; Willett, P.; Glen, R. C.; Leach, A. R.; Taylor, R. *J. Mol. Biol.* **1997**, *267*, 727.
21. Morris, G. M.; Goodsell, D. S.; Halliday, R. S.; Huey, R.; Hart, W. E.; Belew, R. K.; Olson, A. J. *J. Comput. Chem.* **1998**, *19*, 1639.
22. Cozzini, P.; Fornabaio, M.; Marabotti, A.; Abraham, D. J.; Kellogg, G. E.; Mozzarelli, A. *J. Med. Chem.* **2002**, *45*, 2469.
23. Kellogg, G. E.; Abraham, D. J. *Eur. J. Med. Chem.* **2000**, *35*, 651.

24. Spyrakis, F.; Fornabaio, M.; Cozzini, P.; Mozzarelli, A.; Abraham, D. J.; Kellogg, G. E. *J. Am. Chem. Soc.* **2004**, *126*, 11764.
25. Fornabaio, M.; Spyrakis, F.; Mozzarelli, A.; Cozzini, P.; Abraham, D. J.; Kellogg, G. E. *J. Med. Chem.* **2004**, *47*, 4507.
26. Cashman, D. J.; Scarsdale, J. N.; Kellogg, G. E. *Nucleic Acids Res.* **2003**, *31*, 4410.
27. Burnett, J. C.; Botti, P.; Abraham, D. J.; Kellogg, G. E. *Proteins* **2001**, *42*, 355.
28. Amadasi, A.; Spyrakis, F.; Cozzini, P.; Abraham, D. J.; Kellogg, G. E.; Mozzarelli, A. *J. Mol. Biol.* **2006**, *358*, 289.
29. Spyrakis, F.; Cozzini, P.; Bertoli, C.; Marabotti, A.; Kellogg, G. E.; Mozzarelli, A. *BMC Struct. Biol.* **2007**, *7*, 4.
30. Eldridge, M. D.; Murray, C. W.; Auton, T. R.; Paolini, G. V.; Mee, R. P. *J. Comp. Aided Mol. Des.* **1997**, *11*, 425.
31. Kontoyianni, M.; McClellan, L. M.; Sokol, G. S. *J. Med. Chem.* **2004**, *47*, 558.
32. Goodford, P. J. *J. Med. Chem.* **1985**, *28*, 849.
33. Gasteiger, J.; Marsili, M. *Tetrahedron* **1980**, *36*, 3219.
34. Kellogg, G. E.; Burnett, J. C.; Abraham, D. J. *J. Comput. Aided Mol. Des.* **2001**, *15*, 381.
35. Hansch, C.; Leo, A. J. In *Substituent Constants for Correlation Analysis in Chemistry and Biology*; Wiley: New York, N.Y., 1979.